Journal of Biomolecular NMR, 6 (1995) 153–162
ESCOM

J-Bio NMR 287

Spectral density function mapping using ^{15}N relaxation data exclusively

Neil A. Farrow[a], Ouwen Zhang[a], Attila Szabo[b], Dennis A. Torchia[c] and Lewis E. Kay[a]

[a]*Protein Engineering Network of Centres of Excellence and Departments of Medical Genetics, Biochemistry and Chemistry, University of Toronto, Toronto, ON, Canada M5S 1A8*
[b]*Laboratory of Chemical Physics, National Institute of Diabetes and Digestive and Kidney Diseases, National Institutes of Health, Bethesda, MD 20892, U.S.A.*
[c]*Bone Research Branch, National Institute of Dental Research, National Institutes of Health, Bethesda, MD 20892, U.S.A.*

Received 27 January 1995
Accepted 20 March 1995

Keywords: Protein dynamics; Spectral density functions; ^{15}N relaxation

Summary

A method is presented for the determination of values of the spectral density function, J(ω), describing the dynamics of amide bond vectors from ^{15}N relaxation parameters alone. Assuming that the spectral density is given by the sum of Lorentzian functions, the approach allows values of J(ω) to be obtained at $\omega=0$, ω_N and $0.870\omega_H$, where ω_N and ω_H are Larmor frequencies of nitrogen and proton nuclei, respectively, from measurements of ^{15}N T_1, T_2 and ^1H-^{15}N steady-state NOE values at a single spectrometer frequency. Alternatively, when measurements are performed at two different spectrometer frequencies of i and j MHz, J(ω) can be mapped at $\omega=0$, ω_N^i, ω_N^j, $0.870\omega_H^i$ and $0.870\omega_H^j$, where ω_N^i, for example, is the ^{15}N Larmor frequency for a spectrometer operating at i MHz. Additionally, measurements made at two different spectrometer frequencies enable contributions to transverse relaxation from motions on millisecond–microsecond time scales to be evaluated and permit assessment of whether a description of the internal dynamics is consistent with a correlation function consisting of a sum of exponentials. No assumptions about the specific form of the spectral density function describing the dynamics of the ^{15}N-NH bond vector are necessary, provided that $dJ(\omega)/d\omega$ is relatively constant between $\omega=\omega_H+\omega_N$ to $\omega=\omega_H-\omega_N$. Simulations demonstrate that the method is accurate for a wide range of protein motions and correlation times, and experimental data establish the validity of the methodology. Results are presented for a folded and an unfolded form of the N-terminal SH3 domain of the protein drk.

Introduction

The relationship between the internal dynamics of proteins and their biological function has been the subject of much research in recent years. It is widely recognized, for example, that proteins undergo significant motions on a variety of time scales (Karplus and McCammon, 1986) and that important biological processes such as protein folding, enzyme catalysis and protein–ligand interactions all involve motion. Although to date considerable efforts have focused on structural studies of macromolecules, it is clear that a complete description of such systems requires an understanding of the molecular dynamics as well. Heteronuclear NMR relaxation studies have emerged as a powerful approach for the characterization of the motional properties of molecules in solution for a number of reasons (for reviews see Palmer, 1993; Wagner et al., 1993). First, uniform isotopic labelling techniques permit the dynamics of the protein to be characterized at the level of individual residues throughout the molecule. Second, the measurable relaxation parameters provide information about motions over a variety of time scales, ranging from picoseconds to milliseconds. Finally, because the relaxation is dominated by the dipole–dipole interaction between the heteronucleus and the attached proton spin(s), and to a lesser extent by chemical shift anisotropy, it is possible to extract motional properties in a manner which is independent of the structure of the molecule under study (Allerhand et al., 1971).

Extraction of information about the dynamics of a protein from heteronuclear NMR relaxation studies is typically based on the measurement of heteronuclear longitudinal and transverse relaxation rates and the steady-state ^1H-X heteronuclear NOE. These three parameters are sensitive to the motion of the bond connecting the heteronucleus to its attached proton at prescribed fre-

quencies, related to the ^{1}H and X nuclear Larmor frequencies. More specifically, the relaxation parameters are related to the spectral density functions, $J(\omega)$, characterizing the motion of the ^{1}H-X bond at the five frequencies $\omega = 0$, ω_X, ω_H, $\omega_H \pm \omega_X$, where ω_i is the Larmor frequency of spin i. Thus, the three measured relaxation parameters may be thought of as 'sampling' the spectral density function at five frequencies (Abragam, 1961). However, because the sampling occurs at five frequencies and only three parameters are measured, the resulting system of equations is underdetermined and the values of the spectral density function at the five frequencies may not be extracted directly from the measurements without a priori assumptions about the form of $J(\omega)$. One approach to characterize the spectral density function has been to assume an appropriate model for the motion of the bond vector and, on the basis of such a model, to calculate $J(\omega)$ analytically (Woessner, 1962; Kinoshita et al., 1977; London and Avitabile, 1978; Wittebort and Szabo, 1978; Richarz et al., 1980; Brainard and Szabo, 1981). The form of $J(\omega)$ most commonly employed, however, is that of the model-free spectral density function of Lipari and Szabo (1982a,b). The model-free spectral density function is formulated on the assumption that the correlation function describing the dynamics of the amide bond vector may be written as the product of two exponentially decaying correlation functions resulting from the overall tumbling motion of the molecule and the internal motion of the bond vector. In its simplest form, the approach assumes that the macromolecule tumbles isotropically in solution. For an isotropically reorienting molecule, the model-free spectral density is exact as long as all internal motions are in the extreme narrowing limit, independent of any physical model of such motions. Despite the simple form of $J(\omega)$ in this case, this approach has been used successfully to analyze the internal dynamics of a large number of biological molecules (Kay et al., 1989; Clore et al., 1990; Kördel et al., 1992; Schneider et al., 1992; Stone et al., 1992; Cheng et al., 1993). Nevertheless, it would clearly be advantageous to obtain information about the motions of the protein without requiring assumptions relating to the overall tumbling of the molecule or the exact form of the spectral density function.

An alternative approach to characterize the dynamics of a protein, which does not require any assumption about the form of the spectral density function, is the spectral density mapping procedure described by Peng and Wagner (1992a). These authors augment the three measurements described above with measurements of the relaxation rates of I_z, $I_z X_z$ and $I_z X_{tr}$ magnetization, where I_z and X_z are the z components of ^{1}H and X magnetization, respectively, and X_{tr} is transverse X magnetization. Theoretically, these additional measurements permit the exact determination of the values of the spectral density function at all five frequencies described above. However, there are a number of practical problems with such an approach. First, the relaxation of I_z, $I_z X_z$ and $I_z X_{tr}$ is not correctly described by a single exponential decay as assumed in this approach. Second, as the authors indicate, the method relies on taking differences between relaxation rates that are of a similar magnitude and therefore it is sensitive to experimental error. These problems may explain why, in the spectral mapping study of the protein eglin C, negative values of the spectral density function evaluated at high frequencies were obtained for some residues and, in addition, in some cases the spectral density function increased as a function of frequency between 450 and 550 MHz (Peng and Wagner, 1992b).

Keeping in mind the problems associated with the original spectral mapping approach, we describe a new analytical procedure which permits accurate determination of the values of the spectral density function at three frequencies from ^{15}N relaxation parameters measured at a single spectrometer frequency. Alternatively, if measurements are performed at a second spectrometer frequency, it is possible to map the spectral density function at five frequencies. The method relies on the simplification of expressions for ^{15}N relaxation parameters by replacing the linear combinations of the values of the spectral density function evaluated at ω_H and $\omega_H \pm \omega_X$ in expressions for the ^{15}N T_1, T_2 and steady-state ^{1}H-^{15}N NOE with a single equivalent spectral density term. To demonstrate the validity of this methodology, ^{15}N T_1, T_2 and steady-state ^{1}H-^{15}N NOE measurements at 500 and 600 MHz have been performed on uniformly ^{15}N-labelled samples of the 59-amino acid N-terminal SH3 domain of the *Drosophila* signal transduction protein drk (drkN SH3). Studies with drkN SH3 dissolved in 2 M guanidine hydrochloride, in which the protein is completely denatured (Zhang et al., 1994), and in 0.4 M sodium sulfate, which stabilizes the folded form of the protein, have been performed. The values of the spectral density function evaluated at five frequencies have been obtained for each resolvable cross peak in the spectra of both the folded and the unfolded forms of the drkN SH3 domain. The results of the present method demonstrate that in all cases the values of the spectral density function are positive and do not increase as a function of increasing frequency.

Materials and Methods

^{15}N-enriched samples of drkN SH3 were produced as described previously (Zhang et al., 1994). Two separate samples were prepared for the NMR relaxation studies described below. An unfolded form of drkN SH3 was obtained by dissolving the protein in 2.0 M guanidine hydrochloride, while a fully folded form of the protein was produced by dissolving it in 0.4 M sodium sulfate. Both protein samples were prepared to a concentration of 1 mM, pH 6.0, 90% H_2O/10% D_2O.

NMR spectra were recorded at 14 °C on a Varian Unity 500 MHz spectrometer and on a Varian Unity Plus 600 MHz spectrometer. Both spectrometers were equipped with triple-resonance pulsed field gradient probes with actively shielded z-gradients. The enhanced-sensitivity pulse sequences, used to determine T_1, T_2 and steady-state ^1H-^{15}N NOE values with minimal water saturation and dephasing, have been described previously (Farrow et al., 1994). All spectra recorded at 500 MHz were collected as 160×512 complex matrices with sweep widths of 8000 and 1500 Hz in the ^1H and ^{15}N dimensions, respectively. Spectra collected at 600 MHz were acquired as 160×640 complex matrices with sweep widths of 10 000 and 1500 Hz in the ^1H and ^{15}N dimensions, respectively. Spectra for the measurement of T_1 values were recorded with 32 scans per t_1 point and with recycle delays of 1 s. Seven time points were used for each T_1 series, with delays of 0.011 to 0.899 s. Spectra for the measurement of T_2 values of the unfolded (folded) sample were acquired with 8 (16) scans per t_1 point and with recycle delays of 3 (2) s. The long recycle delays employed when collecting T_2 spectra prevent heating of the sample during the CPMG period due to the high concentrations of sodium sulfate and guanidine hydrochloride in the samples. Eight time points were collected for each T_2 series, with delays between 0.016 and 0.187 s. Values of the steady-state NOE were determined from three pairs of spectra, recorded with and without proton saturation. NOE spectra recorded with proton saturation utilized a recycle delay of 5 s, followed by a 3 s period of saturation, while spectra recorded in the absence of saturation employed a recycle delay of 8 s. Proton saturation was achieved by the application of ^1H 120° pulses every 5 ms (Markley et al., 1971). Lorentzian-to-Gaussian apodization functions were applied in both dimensions prior to Fourier transformation. All data were processed using nmrPipe software (Delaglio, 1993) and peak intensities were characterized as volumes using surface fitting routines in nmrPipe.

Results and Discussion

The heteronuclear ^{15}N relaxation times T_1 and T_2 and the steady-state ^1H-^{15}N NOE are principally affected by dipole–dipole and chemical shift anisotropy relaxation mechanisms and are related to the spectral density function $J(\omega)$ of the amide bond vector by the following equations (Abragam, 1961):

$$1/T_1 = (d^2/4)\,[J(\omega_H - \omega_N) + 3J(\omega_N) + 6J(\omega_H + \omega_N)] + c^2 J(\omega_N) \quad (1)$$

$$1/T_2 = (d^2/8)\,[4J(0) + J(\omega_H - \omega_N) + 3J(\omega_N) + 6J(\omega_H) + 6J(\omega_H + \omega_N)] + (c^2/6)\,[3J(\omega_N) + 4J(0)] \quad (2)$$

$$NOE = 1 + (d^2/4)\,(\gamma_H/\gamma_N)\,[6J(\omega_H + \omega_N) - J(\omega_H - \omega_N)]\,T_1 \quad (3)$$

where $d = [\mu_0 h \gamma_N \gamma_H / (8\pi^2)]\,\langle 1/r_{NH}^3 \rangle$, $c = (\omega_N/\sqrt{3})\,(\sigma_\parallel - \sigma_\perp)$, ω_N and ω_H are the Larmor frequencies of the ^{15}N and ^1H nuclei, respectively, μ_0 is the permeability of free space, γ_N and γ_H are the gyromagnetic ratios of ^{15}N and ^1H, h is Planck's constant, r_{NH} is the length of the amide bond vector, and $\sigma_\parallel$ and $\sigma_\perp$ are the parallel and perpendicular components of the assumed axially symmetric chemical shift tensor. When the model-free formalism of Lipari and Szabo (1982a,b) is employed, the spectral density function is given by:

$$J(\omega) = 2/5\,\{S^2 \tau_m / [1 + (\omega^2 \tau_m^2)] + (1 - S^2)\,\tau / [1 + (\omega\tau)^2]\} \quad (4)$$

in which τ_m is the overall correlation time, S^2 is the generalized order parameter, τ_e is the correlation time for internal motions, and $1/\tau = 1/\tau_m + 1/\tau_e$.

In a recent paper we exploited the assumption that the high-frequency spectral density terms that contribute to the relaxation processes are of approximately equal magnitude, i.e., $J(\omega_H \pm \omega_N) \approx J(\omega_H)$, and therefore may be replaced by a single equivalent term, $J(\omega_h)$ (Farrow et al., 1995). Briefly, it was argued that such an assumption is justified by the experimental data of Peng and Wagner (1992a,b) and also by consideration of the form of the model-free spectral density function, which has been used to successfully model relaxation data from a large number of proteins. Under this assumption, Eqs. 1–3 may be recast to yield:

$$J(\omega_h) = [4/(5d^2)]\,(\gamma_N/\gamma_H)\,(NOE - 1)/T_1 \quad (5)$$

$$J(\omega_N) = [1/T_1 - (7d^2/4)\,J(\omega_h)]\,/\,[(3d^2/4) + c^2] \quad (6)$$

$$J(0) = [1/T_2 - (3d^2/8 + c^2/2)\,J(\omega_N) - (13d^2/8)\,J(\omega_h)]\,/\,(d^2/2 + 2c^2/3) \quad (7)$$

Equations 5–7 formally describe the approach that has previously been employed (Farrow et al., 1995) to analyze the relaxation data of a folded/unfolded equilibrium mixture of drkN SH3 in aqueous solution.

While values of the spectral density function may be determined from ^{15}N relaxation measurements using Eqs. 5–7, this approach can be improved. For example, consider the contributions of the values of the spectral density function evaluated at $\omega = \omega_H \pm \omega_N$ in Eq. 3, $6J(\omega_H + \omega_N) - J(\omega_H - \omega_N)$. Assuming a form of the spectral density function given by $J(\omega) = \lambda_1/\omega^2 + \lambda_2$, where the first and second terms represent contributions to $J(\omega)$ from overall rotation and internal dynamics, respectively, and requiring that the relation

$$6J(\omega_H + \omega_N) - J(\omega_H - \omega_N) = AJ(\omega_q) \quad (8)$$

where A is a constant and ω_q is a single 'equivalent' frequency be valid, gives:

$$A = 5 \tag{9a}$$

$$6/(\omega_H+\omega_N)^2 - 1/(\omega_H-\omega_N)^2 = 5/\omega_q^2 \tag{9b}$$

Equation 9b can be recast in terms of the appropriate gyromagnetic ratios, such that:

$$\omega_q = \{5/(6/[1+(\gamma_N/\gamma_H)]^2 - 1/[1-(\gamma_N/\gamma_H)]^2)\}^{1/2}\omega_H = 0.870\omega_H \tag{10}$$

Using arguments similar to those given above, it is straightforward to show that the linear combinations of spectral density terms evaluated at $\omega = \omega_H \pm \omega_N$, ω_H in Eqs. 1, 2 and 3 can be replaced by the relations given in Eqs. 11b, c and a, respectively:

$$6J(\omega_H+\omega_N) - J(\omega_H-\omega_N) = 5J(0.870\omega_H) \tag{11a}$$

$$J(\omega_H-\omega_N) + 6J(\omega_H+\omega_N) = 7J(0.921\omega_H) \tag{11b}$$

$$J(\omega_H-\omega_N) + 6J(\omega_H) + 6J(\omega_H+\omega_N) = 13J(0.955\omega_H) \tag{11c}$$

The assumption that the spectral density function has the form $J(\omega) = \lambda_1/\omega^2 + \lambda_2$ is actually exact if the correlation function describing the dynamics of the amide bond vector is given by a sum of exponentials and provided that $\omega\tau_i \gg 1$, where τ_i are the correlation times describing the overall rotation of the molecule, and $\omega\tau_j \ll 1$, where τ_j are the correlation times describing internal motions. Note that the molecular tumbling need not be isotropic. However, numerical simulations show that for a spectral density function consisting of a sum of Lorentzian functions centered at $\omega = 0$, these results are accurate for all values of $\omega\tau_i$. For example, assuming the form of the spectral density function as described by Lipari and Szabo (1982a, b) (Eq. 4) with τ_m, S^2 and τ_e having the range of values typically found in proteins, namely 2 ns $\le \tau_m \le$, $0.1 \le S^2 \le 1$, 0.001 ns $\le \tau_e \le 1$ ns, the two sides of Eqs. 11a–c differ by no more than 0.8%.

It follows, therefore, that if the conditions described above hold, Eqs. 1–3 can be rewritten as:

$$NOE = 1 + (d^2/4)(\gamma_H/\gamma_N)[5J(0.870\omega_H)]T_1 \tag{12}$$

$$1/T_1 = (d^2/4)[3J(\omega_N) + 7J(0.921\omega_H)] + c^2J(\omega_N) \tag{13}$$

$$1/T_2 = (d^2/8)[4J(0) + 3J(\omega_N) + 13J(0.955\omega_H)] + (c^2/6)[3J(\omega_N) + 4J(0)] \tag{14}$$

The fact that Eqs. 11a–c are satisfied for all $\omega\tau_i$ implies that the errors introduced into the expressions for T_1, T_2 and NOE by this simplification are small. Comparison of Eqs. 5 and 12 shows that $J(\omega_h)$ used in our previous study (Farrow et al., 1995) is in fact equivalent to $J(0.870\omega_H)$. Together, Eqs. 12–14 relate the relaxation parameters, T_1, T_2 and NOE, to the spectral density function at five frequencies, i.e., 0, ω_N, $0.870\omega_H$, $0.921\omega_H$, and $0.955\omega_H$. In practice, the value of $J(0.870\omega_H)$ may be extracted directly from the values of T_1 and NOE using Eq. 12, while the values of $J(0.921\omega_H)$ and $J(0.955\omega_H)$ may be estimated from the value of $J(0.870\omega_H)$ using any one of the three methods listed below. Note that once values of $J(0.921\omega_H)$ and $J(0.955\omega_H)$ are estimated, $J(\omega_N)$ and $J(0)$ can be determined directly from Eqs. 13 and 14.

Method 1

Assume that $J(\omega)$ is effectively constant at $\omega \approx \omega_H$ and therefore that $J(0.921\omega_H)$ and $J(0.955\omega_H)$ may be replaced by the experimentally determined value of $J(0.870\omega_H)$. This approach reduces to the methodology employed in our previous paper (Farrow et al., 1995), but with the reinterpretation of $J(\omega_h)$ as $J(0.870\omega_H)$. Note that this assumption corresponds to the slowest decay of $J(\omega)$ consistent with a Lorentzian form of the spectral density function.

Method 2

Assume that $J(\omega) \propto 1/\omega^2$ and estimate values of $J(0.921\omega_H)$ and $J(0.955\omega_H)$ from $J(0.870\omega_H)$ using the relation $J(\varepsilon\,\omega_H) = (0.870/\varepsilon)^2 J(0.870\omega_H)$, where $\varepsilon = 0.921$ or 0.955. Note that the assumption that $J(\omega) \propto 1/\omega^2$ corresponds to the fastest rate of decay of $J(\omega)$ consistent with a Lorentzian form for the spectral density function. Consequently, within the Lorentzian approximation, Methods 1 and 2 should yield lower and upper bounds for $J(0)$ and $J(\omega_N)$, respectively.

Method 3

If data sets are obtained at two different field strengths, it is possible to extrapolate the values of $J(0.921\omega_H)$ and $J(0.955\omega_H)$ using the following relation:

$$J(\varepsilon\,\omega_H) \approx J(0.870\omega_H) + (\varepsilon - 0.870)\omega_H J'(0.870\omega_H) \tag{15}$$

where $\varepsilon = 0.921$ or 0.955. Equation 15 was derived by a first-order Taylor series expansion of $J(\omega)$ about $J(0.870\omega_H)$, where $J'(0.870\omega_H)$ is the first derivative of $J(\omega)$ evaluated at $\omega = 0.870\omega_H$. This value can be estimated from measurements of $J(0.870\omega_H)$ at the two field strengths (i.e., $J'(0.870\omega_H) \approx [J(0.870\omega_H^i) - J(0.870\omega_H^j)]/[0.870(\omega_H^i - \omega_H^j)]$, where ω_H^i and ω_H^j are the Larmor proton frequencies corresponding to the field strengths at which measurements of $J(0.870\omega_H^i)$ and $J(0.870\omega_H^j)$, respectively, are obtained).

The results described above have been derived assuming that $J(\omega)$ is given by a sum of Lorentzian functions centered at $\omega = 0$ (i.e., that the correlation function is a sum of exponentials). In fact, the results are considerably more general than the above discussion suggests. For example, consider Eq. 8, where the form of $J(\omega)$ is now arbitrary. Expanding the left-hand side of this equation in a Taylor series about ω_H gives, to first order:

$$6J(\omega_H+\omega_N) - J(\omega_H-\omega_N) = 5J(\omega_H) + 7\omega_N J'(\omega_H) \quad (16)$$

where $J'(\omega)$ is the first derivative of J with respect to ω. Setting $\omega_q = \omega_H + \delta$, the right-hand side of Eq. 8 becomes:

$$AJ(\omega_H+\delta) = AJ(\omega_H) + A\delta J'(\omega_H) \quad (17)$$

to first order. In order to satisfy Eq. 8, it is necessary that the right-hand sides of Eqs. 16 and 17 be equivalent. This requires that the values of A and δ be set to 5 and $(7/5)\omega_N$, respectively, from which it follows that $\omega_q = \omega_H[1+(7/5)\gamma_N/\gamma_H]$, Eq. 18a. Similar relations hold for linear combinations of spectral densities evaluated at $\omega = \omega_H$, $\omega_H \pm \omega_N$ in expressions for T_1 and T_2 and are given in Eqs. 18b and c, respectively:

$$\begin{aligned} &6J(\omega_H+\omega_N) - J(\omega_H-\omega_N) \approx \\ &5J(\omega_H[1+(7/5)\gamma_N/\gamma_H]) = 5J(0.858\omega_H) \end{aligned} \quad (18a)$$

$$\begin{aligned} &J(\omega_H-\omega_N) + 6J(\omega_H+\omega_N) \approx \\ &7J(\omega_H[1+(5/7)\gamma_N/\gamma_H]) = 7J(0.928\omega_H) \end{aligned} \quad (18b)$$

$$\begin{aligned} &J(\omega_H-\omega_N) + 6J(\omega_H) + 6J(\omega_H+\omega_N) \approx \\ &13J(\omega_H[1+(5/13)\gamma_N/\gamma_H]) = 13J(0.961\omega_H) \end{aligned} \quad (18c)$$

Note that Eqs. 18a–c are essentially identical to Eqs. 11a–c, with very slight differences arising from the fact that an explicit form of $J(\omega)$ has not been assumed in the derivation of Eq. 18 and an expansion to first order only has been considered. The differences in Eqs. 11 and 18 are well within the experimental errors of relaxation time measurements and, in what follows, the ω_q values of Eq. 11 will be assumed. The assumption that a first-order expansion of $J(\omega)$ about $\omega = \omega_H$ is sufficient to adequately describe $J(\omega_H \pm \omega_N)$ implies that $J(\omega)$ changes slowly from $\omega = \omega_H + \omega_N$ to $\omega = \omega_H - \omega_N$. This will certainly be the case for a spectral density function centered at $\omega = 0$ describing the dynamics of a macromolecule. However, for the case of a spectral density function centered at $\omega_0 \approx \omega_H$, $J'(\omega_H) \approx 0$ and the results of Eq. 18 remain valid in the limit that the width of $J(\omega)$ is much larger than $2\omega_N$.

Equation 12 suggests an experimental approach for assessing whether the observed dynamics can be described by a correlation function consisting of a sum of exponentials with positive coefficients. Measurement of NOE and T_1 values at 500 and 600 MHz permits a straightforward determination of $J(0.870\omega_H)$ at two fields. Clearly, if the form of the spectral density function is a sum of Lorentzian functions, it is expected that $J(0.870\omega_H^{500}) > J(0.870\omega_H^{600})$, where the superscripts denote the frequencies (in MHz) at which the data were collected. Values of $J(\omega)$ which increase with frequency or decay at a rate much greater than $1/\omega^2$ suggest that a description of the motion involves correlation functions which are more complex than simple sums of exponentials.

In order to provide insight into the dynamics of drkN SH3, ^{15}N relaxation parameters have been measured for this system under two different sets of experimental conditions; drkN SH3 dissolved in the presence of either 2.0 M guanidine hydrochloride or 0.4 M sodium sulfate. As mentioned previously, the use of guanidine hydrochloride as a solvent ensures that the protein is completely denatured, while sodium sulfate has been shown to stabilize the folded form of the molecule. Therefore, these solvent conditions give rise to molecules with very different dynamical properties and enable the methodology developed to be tested on protein systems displaying a wide range of motion. Figures 1a and 1b show the values of $J(0.870\omega_H)$ calculated using Eq. 12 from ^{15}N T_1 and steady-state ^1H-^{15}N NOE measurements at $\omega_H = 499.257$ and $\omega_H = 598.953$ MHz for the unfolded and folded forms of drkN SH3, respectively. Errors in the value of $J(0.870\omega_H)$ were determined using a Monte Carlo procedure (Press et al., 1986), taking into account the experimental errors in the measured T_1 and NOE values. Figure 1a clearly shows that for the unfolded protein, the values of J(434.4 MHz) = $J(0.870\omega_H^{499.257})$, measured on a per residue basis, are larger

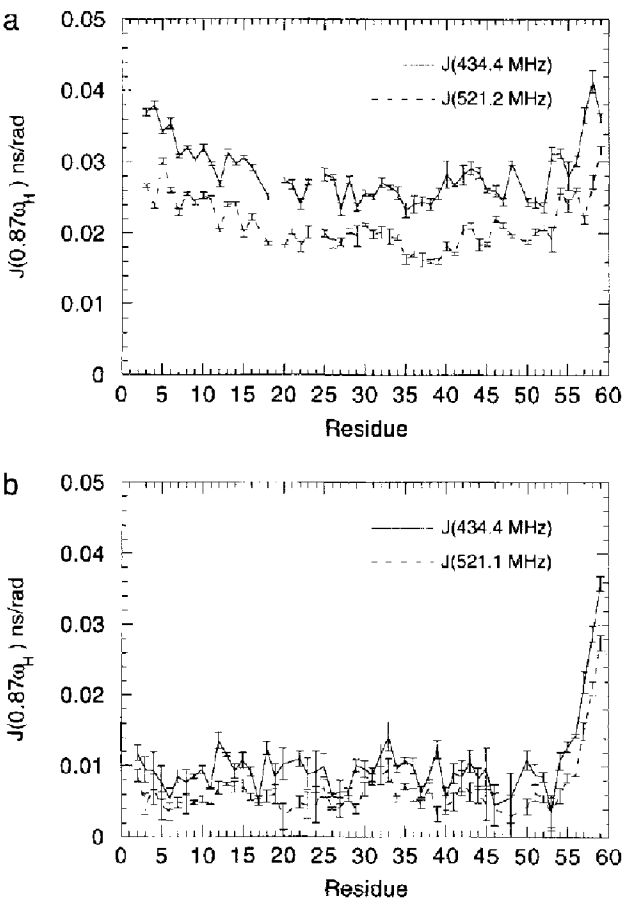

Fig. 1. Plots of $J(0.870\omega_H)$, the spectral density function evaluated at $0.870\omega_H$, versus residue number for (a) the unfolded and (b) the folded form of the drkN SH3 domain. The values of the spectral density function at 434.4 and 521.2 MHz were determined using T_1 and NOE data collected at 499.257 and 598.953 MHz, respectively.

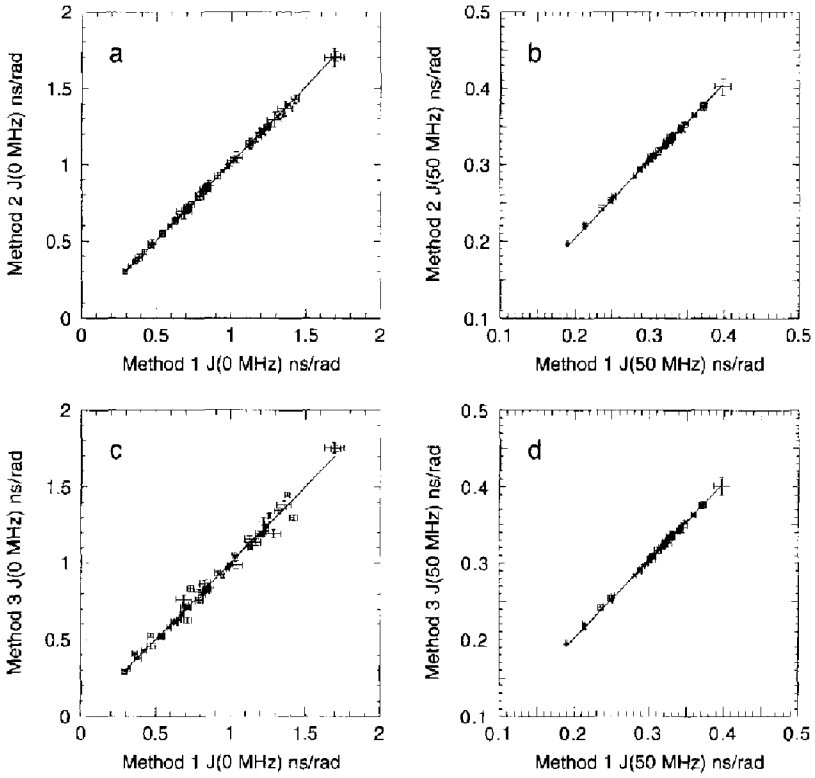

Fig. 2. Comparison of the values of $J(\omega_N)$ and $J(0)$ determined by the three methods used to extract $J(0.921\omega_H)$ and $J(0.955\omega_H)$ from $J(0.870\omega_H)$. (a) Correlation between $J(0)$ values obtained for the unfolded drkN SH3 domain from Methods 1 and 2; (b) correlation between $J(\omega_N)$ values obtained for the unfolded drkN SH3 domain from Methods 1 and 2; (c) correlation between $J(0)$ values obtained for the unfolded drkN SH3 domain from Methods 1 and 3; (d) correlation between $J(\omega_N)$ values obtained for the unfolded drkN SH3 domain from Methods 1 and 3. Parts e–h are identical to a–d, illustrating correlations for the folded drkN SH3 domain. Best fit lines of the form $y = mx$ are shown in each graph, with the values of m ranging from 0.98 (g) to 1.02 (b). For Methods 1 and 2, data collected at 499.257 MHz were employed, while data collected at 499.257 and 598.953 MHz were used for Method 3. Note that the values of $J(\omega_N)$ and $J(0)$ are independent of the method used. $J(0)$ values calculated via Method 3 are averages of values obtained from the 499.257 and 598.953 MHz data, as described in the text. The increased scatter in correlations involving Method 3 reflects the fact that data from two frequencies were used in this method.

than those of $J(521.2\ \text{MHz}) = J(0.870\omega_H^{598.953})$. With the exception of two residues in the folded form of the drkN SH3 domain (Leu^{17} and Ile^{53}), for which values of the spectral density function at the two frequencies appear to be the same to within the measurement error, the spectral density values at 434.4 MHz are higher than those at 521.2 MHz.

A number of simulations have been performed to assess the accuracy to which the method described above determines values of the spectral density function; the results are summarized in Table 1. The values of the relaxation parameters (^{15}N T_1, T_2 and the steady-state ^1H-^{15}N NOE) used in the simulations were calculated using the expressions given in Eqs. 1–3, in conjunction with the model-free spectral density function, Eq. 4, described by Lipari and Szabo (1982a,b). The parameters in the model-free spectral density function were adjusted to simulate three situations: (i) no internal motion of the amide bond vector ($S^2 = 1$, $\tau_e = 0$); (ii) motional properties similar to those found in folded proteins ($S^2 = 0.8$, $\tau_e = 50$ ps); and (iii) motional properties similar to those seen in unfolded proteins or in flexible loop regions of folded proteins ($S^2 = 0.5$, $\tau_e = 500$ ps). Table 1 shows the values of the model-free spectral density function determined at three frequencies, i.e., 0, ω_N and $0.870\omega_H$, for simulated data at 500 MHz and an overall correlation time of 5 ns. The values of the spectral density function extracted by assuming a single value for the high-frequency terms (Eqs. 5–7) are tabulated as 'Method 1' and the values extracted by using the $1/\omega^2$ approximation to determine $J(0.921\omega_H)$ and $J(0.955\omega_H)$ in conjunction with Eqs. 12–14 are tabulated as 'Method 2'. The errors in the table were calculated using a Monte Carlo method (Press et al., 1986), assuming measurement errors for the T_1, T_2 and NOE relaxation parameters of 2%, 2% and 5%, respectively.

Table 1 shows that both Methods 1 and 2 estimate the values of the spectral density function to within experimental error for all three levels of protein dynamics considered. As expected, estimating the values of the spectral density function at $0.921\omega_H$ and $0.955\omega_H$ from the value of $J(0.870\omega_H)$ improves the accuracy by which the values of $J(\omega_N)$ and $J(0)$ are determined. Not surprisingly, the values of $J(0)$ and $J(\omega_N)$ become slightly less well determined as the degree of internal motion increases, since the

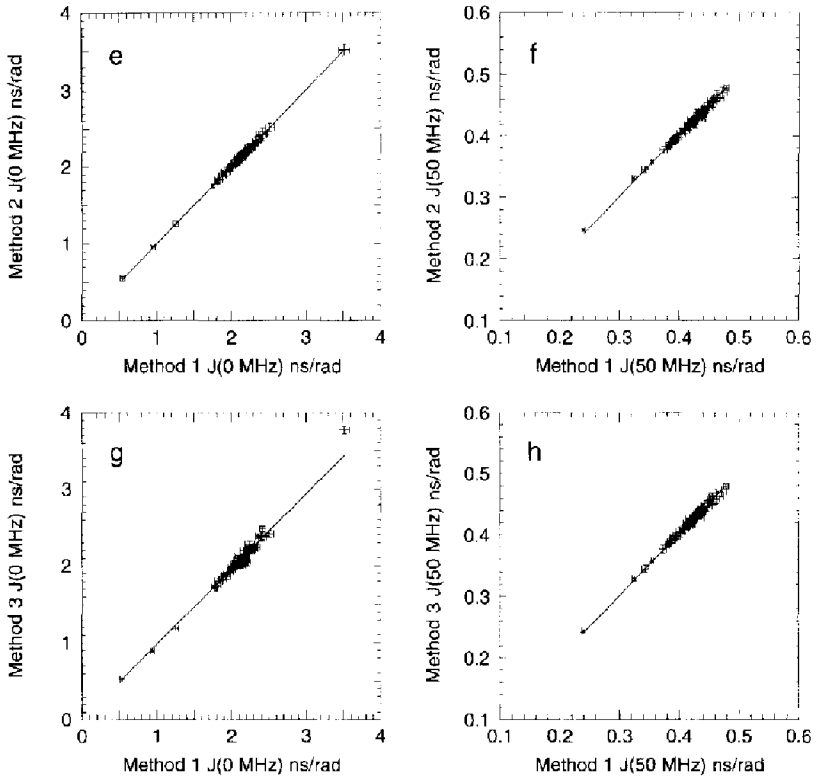

Fig. 2. (continued).

assumed $1/\omega^2$ decay of the spectral density function becomes less exact. However, in all cases the errors in the determined values of $J(\omega)$ are less than 1%. The results of Table I indicate that the approach that we have previously taken (Farrow et al., 1995) in assuming $J(\omega_H \pm \omega_N) \approx J(\omega_H)$, and setting these terms equal to a single term $J(\omega_h)$, is valid for extracting values of $J(\omega_N)$ and $J(0)$, while the present work establishes that $J(\omega_h) = J(0.870\omega_H)$.

The experimental results obtained for drkN SH3 can also be used to establish that the values of $J(\omega_N)$ and $J(0)$ are essentially independent of the method used to determine the values of $J(0.921\omega_H)$ and $J(0.955\omega_H)$. Figures 2a and 2b show the correlation between $J(0)$ and $J(\omega_N)$ values, respectively, obtained for the unfolded drkN SH3 domain from Methods 1 and 2, while Figs. 2c and 2d illustrate the correlation between $J(0)$ and $J(\omega_N)$ values, respectively, obtained via Methods 1 and 3. Similar results for the folded domain are illustrated in Figs. 2e–h. Note that essentially identical values of $J(\omega_N)$ and $J(0)$ are obtained, in a manner independent of which of Methods 1–3 are employed. It bears repeating that, since the two forms of drkN SH3 considered display very different

TABLE I
VALUES OF THE SPECTRAL DENSITY FUNCTION DETERMINED FROM SIMULATED 500 MHz ^{15}N RELAXATION DATA[a]

Model-free parameters / Method	J(0)	$J(\omega_N)$	$J(0.870\omega_H)$
$S^2 = 1.0$; $\tau_e = 0.00$	2.00000	0.56565	0.01065
Method 1	1.99683 (0.04796)	0.56347 (0.01154)	0.01065 (0.00170)
Method 2	2.00001 (0.04943)	0.56566 (0.01190)	0.01065 (0.00166)
$S^2 = 0.8$; $\tau_e = 0.05$	1.60396	0.45648	0.01241
Method 1	1.60139 (0.03955)	0.45471 (0.00950)	0.01241 (0.00139)
Method 2	1.60510 (0.04021)	0.45726 (0.00956)	0.01241 (0.00134)
$S^2 = 0.5$; $\tau_e = 0.50$	1.09091	0.37187	0.04107
Method 1	1.08187 (0.02978)	0.36542 (0.00769)	0.04131 (0.00152)
Method 2	1.09420 (0.03130)	0.37390 (0.00765)	0.04131 (0.00152)

[a] The values of the spectral density function (ns/rad) are reported at zero frequency, J(0), the ^{15}N Larmor frequency, $J(\omega_N)$, and $J(0.870\omega_H)$ (see Eq. 12). The differences between Methods 1 and 2 are described in the text. For each simulation, the model-free parameters used to generate the simulated relaxation data and the associated values of the model-free spectral density function are indicated. An isotropic overall correlation time of 5 ns was used for all simulations. The values in parentheses are the estimated errors in $J(\omega)$, assuming uncertainties of 2%, 2% and 5% in the values of T_1, T_2 and the ^{1}H-^{15}N NOE, respectively.

dynamical behavior, encompassing the range of motions that can be expected in most proteins, the results described here will certainly hold for a great many other systems as well.

The accurate determination of J(0) values is complicated because the measured transverse relaxation times are sensitive to motions on millisecond to microsecond time scales. Such motions reduce the values of T_2 and are manifest as erroneously high values of J(0) when using Methods 1–3 discussed above or the spectral density mapping approach described by Peng and Wagner. Because the contributions of these motions to the line width increase with the square of the spectrometer frequency (Carrington and McLachlan, 1967), the measurement of transverse relaxation times at a second frequency provides a means by which exchange contributions can be quantified. The additional information provided by data measured at a second frequency may be included in the formalism described above and the contribution of the slower motions may be established. For example, from measurements of T_1, T_2 and the steady-state ^1H-^{15}N NOE at 500 and 600 MHz, the methodology discussed above permits the determination of values of J(0), J(50 MHz), J(60 MHz), J(435 MHz) and J(522 MHz), as well as an additional term, R_{ex}. The latter term represents the contribution of millisecond to microsecond time scale motions to the transverse relaxation rate measured at 500 MHz. The values of J(0) and R_{ex} are given by:

$$\begin{aligned} J(0) = (1/\beta)\{&[1/T_2^{600} - \kappa\, 1/T_2^{500}] \\ &- (3d^2/8)[J(\omega_N^{600}) - \kappa\, J(\omega_N^{500})] \\ &- (c_{600}^2/2)[J(\omega_N^{600}) - J(\omega_N^{500})] \\ &- (13d^2/8)[J(0.955\omega_H^{600}) - \kappa\, J(0.955\omega_H^{500})]\} \end{aligned} \quad (19)$$

$$\begin{aligned} R_{ex} = {}& 1/T_2^{500} - (d^2/2 + 2c_{500}^2/3)J(0) \\ &- (3d^2/8 + c_{500}^2/2)\, J(\omega_N^{500}) \\ &- (13d^2/8)\, J(0.955\omega_H^{500}) \end{aligned} \quad (20)$$

where $\kappa = (\omega_H^{600}/\omega_H^{500})^2$, $\beta = (d^2/2)(1-\kappa)$ and the subscripts/superscripts denote the frequency of the spectrometer for which an experimental parameter or frequency was determined; d is defined as for Eqs. 1–3. The constant c_i is equivalent to the constant c in Eqs. 1–3, evaluated at a spectrometer frequency of i MHz. Note that Eqs. 19 and 20 are derived from Eq. 14 and thus contain contributions from the spectral density function evaluated at $0.955\omega_H$, J(477.5 MHz) and J(573 MHz) for data recorded at 500 and 600 MHz, respectively. The values of the spectral density function at these frequencies may be estimated using any of the three methods described previously. In addition, the values of $J(\omega_N^i)$ in Eqs. 19 and 20 are calculated from Eq. 13, as before.

Table 2 shows the results of simulations that utilize data at two spectrometer frequencies, i.e., 500 and 600 MHz. The simulations compare J(0) values calculated using the model-free spectral density function with values extracted using Eqs. 12, 13, 19 and 20 (referred to as Method 2-R_{ex} in the table), and the previously defined Method 2. Different degrees of protein internal motion were simulated by adjusting the model-free spectral density function parameters as described in Table 1. However, because the measurement of T_2 at a second frequency permits estimation of exchange contributions to the measured T_2 value, we have also included three additional simulations in which an R_{ex} term of 0.5 s^{-1} (0.72 $s^{-1} = \kappa 0.5$ s^{-1}) was included in the 500 (600) MHz T_2 data. Values of R_{ex} on this order are typical of those often required to fit protein relaxation data (Stone et al., 1992; Akke et al., 1993; Farrow et al., 1994). As described previously, the presence of non-zero R_{ex} terms will affect the determination of J(0) when data from a single spectrometer only are analyzed. To assess the magnitude of such errors, the values of J(0) estimated using a single frequency and $R_{ex} = 0$ (Method 2) are also shown in Table 2. The methods and uncertainties used to estimate the errors in the values of the spectral densities are as described above for Table 1.

TABLE 2
COMPARISON OF METHODS FOR THE DETERMINATION OF THE SPECTRAL DENSITY FUNCTION AT ZERO FREQUENCY[a]

Model-free parameters / Method	J(0) (ns/rad)	R_{ex} (s^{-1})
$S^2 = 1.0$; $\tau_e = 0.00$	2.00000	0.0000
Method 2	2.00001 (0.04918)	n.d.
Method 2–R_{ex}	2.00004 (0.24009)	−0.0001 (0.6439)
$S^2 = 1.0$; $\tau_e = 0.00$	2.00000	0.5000
Method 2	2.15742 (0.05375)	n.d.
Method 2–R_{ex}	2.00003 (0.26671)	0.4999 (0.7149)
$S^2 = 0.8$; $\tau_e = 0.05$	1.60396	0.0000
Method 2	1.60510 (0.03877)	n.d.
Method 2–R_{ex}	1.60540 (0.19057)	−0.0010 (0.5107)
$S^2 = 0.8$; $\tau_e = 0.05$	1.60396	0.5000
Method 2	1.76253 (0.04400)	n.d.
Method 2–R_{ex}	1.60543 (0.21564)	0.4990 (0.5753)
$S^2 = 0.5$; $\tau_e = 0.50$	1.09091	0.0000
Method 2	1.09420 (0.03043)	n.d.
Method 2–R_{ex}	1.09854 (0.15140)	−0.0138 (0.4047)
$S^2 = 0.5$; $\tau_e = 0.50$	1.09091	0.5000
Method 2	1.25162 (0.03296)	n.d.
Method 2–R_{ex}	1.09855 (0.16152)	0.4862 (0.4332)

[a] Method 2 uses 500 MHz data alone, Method 2–R_{ex} uses data at both 500 and 600 MHz. The value of the spectral density function at zero frequency, J(0), is reported in ns/rad. R_{ex} represents the contribution of millisecond–microsecond time scale motions to the transverse relaxation time, T_2, at 500 MHz. An isotropic overall correlation time of 5 ns was used for all simulations. The values in parentheses are the estimated errors in J(ω), assuming uncertainties of 2%, 2% and 5% in the values of T_1, T_2 and the ^1H-^{15}N NOE, respectively.

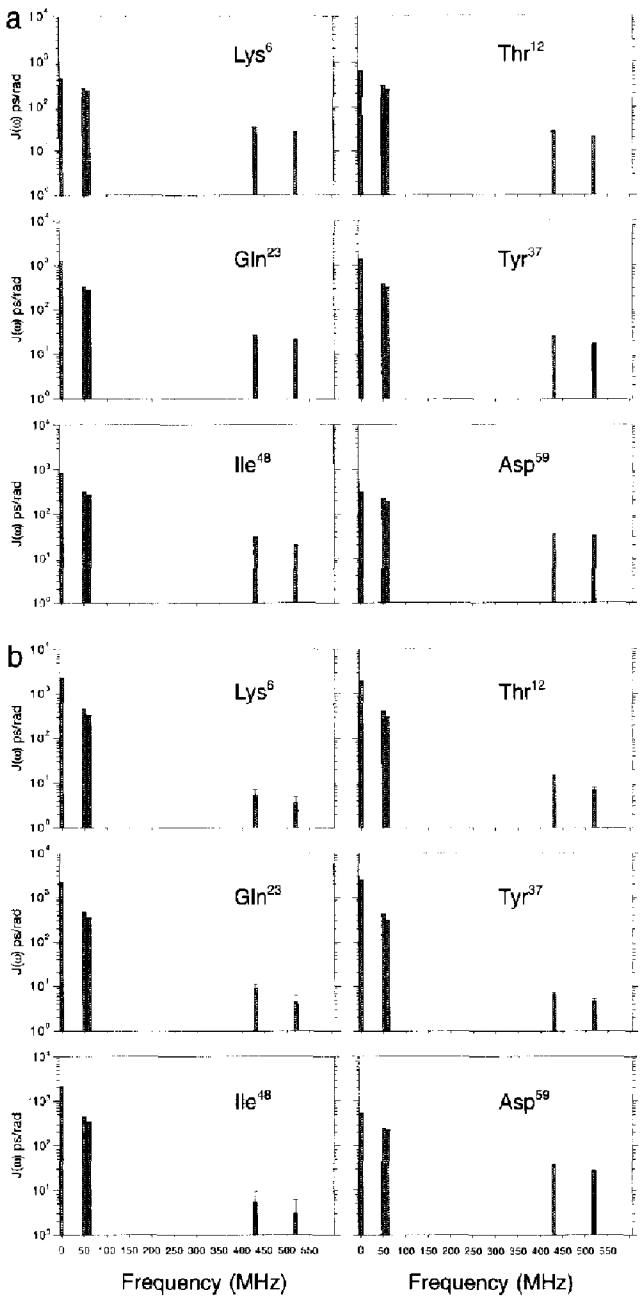

Fig. 3. Values of the spectral density function determined for selected residues from the (a) unfolded and (b) folded states of the drkN SH3 domain. The spectral density function is sampled at five frequencies, i.e., 0, 50.6, 60.7, 434.4, and 521.2 MHz. The latter four values correspond to the frequencies ω_N and $0.870\omega_H$ for the 500 and 600 MHz spectrometers used to measure the relaxation parameters. Note that a log scale is used for the ordinate axis.

The data in Table 2 illustrate that in the absence of contributions from exchange, J(0) values are determined accurately using either Method 2 or Method 2-R_{ex}. It is interesting to note that the simulations indicate that for $R_{ex}=0$ the values of J(0) are determined with slightly higher accuracy when data from 500 MHz alone are used. This is a reflection of the fact that the relation $J(\omega) \propto 1/\omega^2$, used to extrapolate $J(0.955\omega_H)$ from $J(0.870\omega_H)$, is slightly less accurate for data obtained at 600 MHz than at 500 MHz. When data at two fields are employed, the value of J(0) is effectively an average of the values determined at 500 and 600 MHz and the value of J(0) from 600 MHz data alone is determined slightly less accurately than that from exclusively 500 MHz data.

The benefits of using data recorded at two frequencies are seen in the simulations that include a nonzero value for R_{ex}. The inclusion of an R_{ex} term of 0.5 s^{-1} in the simulated T_2 data results in overestimates ranging from 7.9 to 14.7% when J(0) is determined using data measured at 500 MHz only. In contrast, using data recorded at two frequencies, the value of J(0) can be measured to within 1% in all three situations examined. The uncertainties in the values of J(0) determined from data at two frequencies are in all cases significantly larger than those obtained when data from only a single frequency are considered. The larger errors are related to the fact that for macromolecules, the transverse relaxation rate is relatively insensitive to field strength and J(0) values are determined from the difference between values of T_2 at two field strengths (see Eq. 19). The resulting J(0) values are therefore less precise (but far more accurate) than values obtained from a single field.

Figure 3 shows the values of the spectral density function measured for both the folded and the unfolded forms of the drkN SH3 domain derived from ^{15}N T_1, T_2 and steady-state NOE relaxation parameters measured at 500 and 600 MHz. Because the T_2 values measured at the two field strengths are the same to within experimental error for the six residues shown, the values of the spectral density function were determined using the procedure referred to as Method 2 above, i.e., considering the data collected at the two frequencies separately. Very similar values for J(0) are obtained when Method 2-R_{ex} is employed. Values of the spectral density function are determined at the frequencies ω_N and $0.870\omega_H$ for both the 500 and 600 MHz data. Additionally, the value of J(0) is established from each of the data sets and the average of these two measurements is shown in Fig. 3. The data in the figure indicate that there are significant differences in the dynamic behavior of different residues within the protein, with particularly large variations in the values of J(0) observed. The expected decrease in $J(\omega)$ with increasing ω is found to hold for the six residues illustrated in the figure, and in fact for all of the residues in both the folded and the unfolded states of the protein, with the exception of Leu^{17} and Ile^{53} in the folded state, where the values of $J(0.870\omega_H)$ determined from the 500 and 600 MHz data are the same to within experimental error.

Conclusions

Our main results can be summarized as follows:

(1) The method presented allows the extraction of J(0), $J(\omega_N)$ and $J(0.870\omega_H)$ from ^{15}N T_1, T_2 and steady-state ^1H-

^{15}N NOE values measured at a single frequency. The value of $J(0.870\omega_H)$ is obtained directly from the T_1 and NOE values according to Eq. 12. However, $J(0)$ and $J(\omega_N)$ are estimated (Eqs. 13 and 14) only after values of $J(0.921\omega_H)$ and $J(0.955\omega_H)$ have been established. These high-frequency terms can be obtained by setting the values of $J(0.921\omega_H)$ and $J(0.955\omega_H)$ to the experimentally determined value of $J(0.870\omega_H)$ (Method 1) or by a $1/\omega^2$ approximation (Method 2) to estimate values of $J(\omega)$ at $\omega = 0.921\omega_H$ and $0.955\omega_H$ from the value determined at $\omega = 0.870\omega_H$. It has been demonstrated that the details of the estimation of $J(0.921\omega_H)$ and $J(0.955\omega_H)$ have little influence on the accuracy of $J(0)$ and $J(\omega_N)$. Note that the value of $J(0)$ may well contain contributions from motions on millisecond to microsecond time scales, which increase the rate of transverse relaxation.

(2) When data at two separate frequencies are obtained, five values of $J(\omega)$ can be determined as well as an estimate of the contributions to $J(0)$ from exchange. Moreover, data recorded at two separate frequencies provide an opportunity to assess whether a correlation function consisting of a sum of exponentials is consistent with the observed dynamics. In addition, there is now a third option for extrapolation of values of $J(0.921\omega_H)$ and $J(0.955\omega_H)$ from $J(0.870\omega_H)$; namely, these values may be estimated from the value of $J(0.870\omega_H)$ using the linear interpolation given in Eq. 15.

Numerical simulations have established that the methodology described above provides a reliable approach for extracting spectral density values of ^{15}N-NH bond vectors in proteins exhibiting a wide range of motions. Experimental data collected at 500 and 600 MHz on both a folded and an unfolded drkN SH3 domain demonstrate the expected decrease in $J(\omega)$ with increasing frequency and establish that the values of $J(0)$ and $J(\omega_N)$ are essentially independent of the method used to extrapolate $J(0.921\omega_H)$ and $J(0.955\omega_H)$. It should be emphasized that the methods proposed here do not require that the explicit form of the spectral density function be known, nor that the overall molecular tumbling be isotropic. The methods described require only the conservative assumption that the spectral density function varies slowly as a function of frequency between $\omega = \omega_H + \omega_N$ and $\omega = \omega_H - \omega_N$ (Eqs. 16–18). The approach described has been extremely useful in the analysis of relaxation data derived from the unfolded drkN SH3 domain, where simple models of the dynamics are unlikely to be correct.

Acknowledgements

This work was supported through grants from the Natural Sciences and Engineering Research Council of Canada and the National Cancer Institute of Canada, with funds from the Canadian Cancer Society. N.A.F. is a Research Fellow of the National Cancer Institute of Canada, supported with funds provided by the Canadian Cancer Society. O.Z. acknowledges a graduate fellowship from the University of Toronto.

References

Abragam, A. (1961) *Principles of Nuclear Magnetism*, Clarendon Press, Oxford.

Akke, M., Skelton, N.J., Kördel, J., Palmer III, A.G. and Chazin, W.J. (1993) *Biochemistry*, **32**, 9832–9844.

Allerhand, A., Doddrell, D., Glushko, V., Cochran, D.W., Wenkert, E., Lawson, P.J. and Gurd, F.R.N. (1971) *J. Am. Chem. Soc.*, **93**, 544–566.

Brainard, J.R. and Szabo, A. (1981) *Biochemistry*, **20**, 4618–4628.

Carrington, A. and McLachlan, A.D. (1967) *Introduction to Magnetic Resonance*, Harper, New York, NY.

Cheng, J.-W., Lepre, C.A., Chambers, S.P., Fulghum, J.R., Thomson, J.A. and Moore, J.M. (1993) *Biochemistry*, **32**, 9000 9010.

Clore, G.M., Driscoll, P.C., Wingfield, P.T. and Gronenborn, A.M. (1990) *Biochemistry*, **29**, 7387–7401.

Delaglio, F. (1993) *NMRPipe* Software System, National Institutes of Health, Bethesda, MD.

Farrow, N.A., Muhandiram, R., Singer, A.U., Pascal, S.M., Kay, C.M., Gish, G., Shoelson, S.E., Pawson, T., Forman-Kay, J.D. and Kay, L.E. (1994) *Biochemistry*, **33**, 5984–6003.

Farrow, N.A., Zhang, O., Forman-Kay, J.D. and Kay, L.E. (1995) *Biochemistry*, **34**, 868–878.

Karplus, M. and McCammon, J.A. (1986) *Sci. Am.*, **254**, 42–51.

Kay, L.E., Torchia, D.A. and Bax, A. (1989) *Biochemistry*, **28**, 8972–8979.

Kinoshita, K., Kawato., W. and Ikegami, A. (1977) *Biophys. J.*, **20**, 289.

Kördel, J., Skelton, N.J., Akke, M., Palmer III, A.G. and Chazin, W.J. (1992) *Biochemistry*, **31**, 4856–4866.

Lipari, G. and Szabo, A. (1982a) *J. Am. Chem. Soc.*, **104**, 4546–4559.

Lipari, G. and Szabo, A. (1982b) *J. Am. Chem. Soc.*, **104**, 4559–4570.

London, R.E. and Avitabile, J. (1978) *J. Am. Chem. Soc.*, **100**, 7159 7165.

Markley, J.L., Horsley, W.J. and Klein, M.P. (1971) *J. Chem. Phys.*, **55**, 3604–3605.

Palmer III, A.G. (1993) *Curr. Opin. Biotechnol.*, **4**, 385–391.

Peng, J.W. and Wagner, G. (1992a) *J. Magn. Reson.*, **98**, 308–332.

Peng, J.W. and Wagner, G. (1992b) *Biochemistry*, **31**, 8571–8586.

Press, W.H., Flannery, B.P., Teukolsky, S.A. and Vetterling, W.T. (1986) *Numerical Recipes*, Cambridge University Press, Cambridge, p. 548.

Richarz, R., Nagayama, K. and Wüthrich, K. (1980) *Biochemistry*, **19**, 5189–5196.

Schneider, D.M., Dellwo, M.J. and Wand, A.J. (1992) *Biochemistry*, **31**, 3645–3652.

Stone, M.J., Fairbrother, W.J., Palmer III, A.G., Reizer, J., Saier Jr., M.H. and Wright, P.E. (1992) *Biochemistry*, **31**, 4394–4406.

Wagner, G., Hyberts, S. and Peng, J.W. (1993) In *NMR of Proteins* (Eds, Clore, G.M. and Gronenborn, A.M.), Macmillan Press, London, pp. 220–257.

Wittebort, R.J. and Szabo, A. (1978) *J. Chem. Phys.*, **69**, 1722 1736.

Woessner, D.E. (1962) *J. Chem. Phys.*, **36**, 647–654.

Zhang, O., Kay, L.E., Olivier, J.P. and Forman-Kay, J.D. (1994) *J. Biomol. NMR*, **4**, 845 858.